

Journal Pre-proof

Trans-Resveratrol-Loaded Nanostructured Lipid Carrier Formulations for Pulmonary Drug Delivery Using Medical Nebulizers

Iftikhar Khan , Maria Sabu , Nozad Hussein , Huner Omer ,
Chahinez Houacine , Wasiq Khan , Abdelbary Elhissi ,
Sakib Yousaf

PII: S0022-3549(25)00171-6
DOI: <https://doi.org/10.1016/j.xphs.2025.103713>
Reference: XPHS 103713



To appear in: *Journal of Pharmaceutical Sciences*

Received date: 15 October 2024
Revised date: 14 February 2025
Accepted date: 25 February 2025

Please cite this article as: Iftikhar Khan , Maria Sabu , Nozad Hussein , Huner Omer , Chahinez Houacine , Wasiq Khan , Abdelbary Elhissi , Sakib Yousaf , Trans-Resveratrol-Loaded Nanostructured Lipid Carrier Formulations for Pulmonary Drug Delivery Using Medical Nebulizers, *Journal of Pharmaceutical Sciences* (2025), doi: <https://doi.org/10.1016/j.xphs.2025.103713>

This is a PDF file of an article that has undergone enhancements after acceptance, such as the addition of a cover page and metadata, and formatting for readability, but it is not yet the definitive version of record. This version will undergo additional copyediting, typesetting and review before it is published in its final form, but we are providing this version to give early visibility of the article. Please note that, during the production process, errors may be discovered which could affect the content, and all legal disclaimers that apply to the journal pertain.

© 2025 Published by Elsevier Inc. on behalf of American Pharmacists Association.

Trans-Resveratrol-Loaded Nanostructured Lipid Carrier Formulations for Pulmonary Drug Delivery Using Medical Nebulizers

Iftikhar Khan^{1*}, Maria Sabu¹, Nozad Hussein², Huner Omer², Chahinez Houacine³, Wasiaq Khan⁴, Abdelbary Elhissi⁵, Sakib Yousaf¹

¹School of Pharmacy and Biomolecular Sciences, Liverpool John Moores University, Liverpool L3 3AF, United Kingdom

²College of pharmacy, Hawler Medical University, Erbil, Iraq

³School of Pharmacy and Biomedical Sciences, University of Central Lancashire, Preston, PR1 2HE, United Kingdom

⁴Faculty of Engineering and Technology, Liverpool John Moores University, Liverpool L3 3AF, United Kingdom

⁵Department of Pharmaceutical Sciences, College of Pharmacy, QU Health, Qatar University, Doha, Qatar

Corresponding authors:

*Iftikhar Khan

School of Pharmacy and Biomolecular Sciences,

Liverpool John Moores University,

Liverpool L3 3AF,

United Kingdom

Tel: (+44) 151 231 2736

E-mail: I.Khan@ljmu.ac.uk, iftikharkhans@yahoo.com

Abstract

Aerosolization is a non-invasive approach of delivering drugs for both localized and systemic effects, specifically pulmonary targeting. The aim of this study was to deliver trans-resveratrol (TR) as an anti-cancer drug entrapped in a new generation versatile carriers nanostructured lipid carrier (NLC) to protect degradation and improve bioavailability *via* medical nebulizers. Twelve TR-NLC (i.e., F1-F12) formulations were prepared using different combinations and ratios of formulation ingredients *via* hot high-pressure homogenization. Upon analysis, formulations F1 and F2 demonstrated a particle size of <185 nm, a polydispersity index (PDI) <0.25, Zeta potential values of ~30 mV and an entrapment efficiency >94%. The aerosolization performance of the F1 and F2 formulations was performed *via* a next generation impactor (NGI), using medical nebulizers. The air jet nebulizer demonstrated lower drug deposition in the earlier stages (1-2) and significantly higher deposition in the latter stages 3-5 (for both formulations), targeting middle to lower lung deposition. Moreover, the air jet nebulizer exhibited significantly higher emitted dose (ED) ($87.44 \pm 3.36\%$), fine particle dose (FPD) ($1652.52 \pm 9.68 \mu\text{g}$) fine particle fraction (FPF) ($36.25 \pm 4.26\%$), and respirable fraction (RF) ($93.41 \pm 4.03\%$) when the F1 formulation was used as compared to the F2 formulation. Thus, the TR-NLC F1 formulation and air jet nebulizer were identified as the best combination for the delivery and targeting peripheral lungs.

Key words: Medical nebulizer; Pulmonary system; Drug delivery; Liquid lipid; Solid lipid; Cancer.

Introduction

The pulmonary system remains a sought route of drug delivery. This is attributed to the large surface area (100 m²) offered by the lungs, protection from 1st pass metabolism and non-invasive nature of administration [1, 2]. At around one in six fatalities, cancer is one of the main causes of death globally [3, 4]. Lung cancer has one of the worst survival rates when compared to other cancer types, accounting for about 1.8 million deaths per year [5]. Based on the histology, lung cancer is divided into small cell lung cancer (SCLC), non-small cell lung cancer (NSCLC), mesothelioma, sarcoma, and carcinoid. NSCLC makes up more than 85% of all instances of lung cancer and is the most prevalent kind. The bronchi are usually where SCLC starts, but NSCLC can start in any of the many kinds of lung-lining epithelial cells [6, 7]. Surgery, chemotherapy, radiation therapy, and/or immunotherapy are all part of the standard treatment for lung cancer [8]. Additionally, conventional treatments may harm adjacent healthy tissue, which could have a number of negative impacts on patients. New techniques for directing medications to tumour sites can be created with nanotechnology, improving the medication's effectiveness and minimizing its negative effects on healthy tissue.

Nanoparticles [9, 10] possessing the ability for deep lung deposition to exert therapeutic effect, thus have achieved noticeable attention in drug delivery and cancer treatment. Nanoparticles are divided into many sub-classes, including polymeric nanoparticles [11, 12], micelles [13, 14], liposomes/proliposomes [15-17], ethosomes [18, 19], transfersomes/protransfersomes [20, 21], hybrid nanoparticles [22, 23], solid lipid nanoparticles [24, 25], and NLCs [26, 27]. These formulations can deliver both lipophilic and lipophobic drugs, demonstrating very low toxicity in comparison to conventional treatments (e.g., chemotherapy and radiation). These formulations have successfully prolonged drug action either by enhancing the drug half-life or extending the time of drug release. For targeting drug delivery, pH sensitivity is also important, so that active compounds may be released in a particular pH setting [28]. However, it is important to note that each formulation differs with respect to its composition and method of preparation. Among these drug delivery systems, most of the suspension formulations are not stable due to the oxidation and hydrolysis of their phospholipids and are attributed to the agglomeration and leakage of entrapped drugs, resulting in a shorter shelf-life [21, 29]. However, their dry powder formulations are more stable and can be converted into suspensions upon hydration. SLNs possess higher drug entrapment, but due to their perfect crystalline matrix, they may cause drug leakage. Therefore, amongst these nanoparticles, NLC is a new generation formulation, possessing both solid and liquid lipid in the internal core and surfactant to form the outer layer. Moreover, the presence of both the liquid lipid and solid lipid may form an imperfect internal core, which is advantageous in terms of high drug loading and long-term stability as compared to counterpart nanoparticles.

Resveratrol (a novel anti-cancer agent) is a stilbenoid polyphenol with two phenol rings connected by an ethylene bridge [30]. Two isomeric variants of resveratrol have been identified: cis- and trans-resveratrol.

Amongst these two, trans-resveratrol (TR) notably induces cellular responses such as cell cycle arrest, differentiation, apoptosis, and enhances cancer cell anti-proliferation [31, 32]. A combination of NLCs and TR as an anti-cancer drug delivery system may result in better *in-vivo* absorption and bioavailability when compared to TR alone. It is important to know that there have been many preclinical investigations on resveratrol's anticancer properties, but translational research and clinical trials have progressed very little. Most of the research has concentrated on its cellular processes, signal transduction pathways, and anticancer effects both *in vitro* and *in vivo*. A research study conducted by Boocock et al. demonstrated the oral administration of various doses (0.5, 1, 2.5, and 5 g) in humans, where the highest dose demonstrated a recovery of 2.4 μM in the plasma after 1.5 h [33]. In another dose-dependent study where multiple daily doses of 0.5, 1, 2.5 and 5 g were tested in humans for 29 days, the recovered maximum plasma concentration was 4.25 μM [34]. Moreover, in another study where Zhu et al. administered a dose of 50 mg twice a day for 12 weeks, they found a 2.9 μM mean plasma concentration and demonstrated an effect on cancer biomarkers [35].

Pulmonary drug delivery of NLC formulations may be achieved through the use of nebulizers. Upon nebulization, the drug is inhaled through a mouthpiece or facemask with normal tidal breathing, depositing formulations into the deep lungs. There are three main types of medical nebulizers available that have been extensively used for the delivery of lipid-based formulations: air jet, vibrating mesh, and ultrasonic nebulizers [36, 37]. Each nebulizer type consists of many sub-types, possessing the same working principle but with minor modifications in terms of their design. Air jet nebulizers are employed with pressure or compressor systems from which high velocity compressed air is passed through a nebulizer and converts aqueous suspensions or solutions into aerosols. Upon passing the compressed air through the venturi nozzle of the air jet nebulizer, it develops a negative pressure over the formulation, generating inhalable aerosol droplets (which is also called the Bernoulli effect) [2, 38]. Moreover, surface tension of formulations and impaction on the baffle may also help droplet formation in the air jet nebulizers, followed by droplets passing through the mouthpiece for inhalation [39]. Ultrasonic nebulizers have an incorporated piezoelectric crystal, which, upon connecting to a power supply, generates vibration at high frequencies (1-3 MHz) creating energy. This energy either generates a fountain (capillary wave formation) or bubble (cavitational bubble formation) in the stagnant formulation to produce inhalable droplets [40]. Vibrating mesh nebulizers contain a perforated mesh plate, piezoelectric crystal, and a horn transducer. Piezoelectric crystals create vibrations that are transmitted to the connected horn transducer in order to extrude formulations from the perforated mesh plate to produce inhalable droplets [36]. The deposition of aerosol particles/droplets is pertinent to the combined effect of inertial impaction, sedimentation and Brownian diffusion, providing a representative simulation of lung deposition [2, 41]. The *in-vitro* assessment of the aerodynamic diameter of aerosol particles released from the nebulizers can be analysed *via* a next generation impactor (NGI).

This work aimed to combine formulation excipients in various ratios to prepare NLC formulations. This was followed by their characterization and nebulization performance using medical nebulizers (air jet and ultrasonic) for drug deposition in an *in-vitro* lung model. Physicochemical properties (particle size, PDI, Zeta potential and entrapment efficiency) were examined and compared between freshly prepared and stored formulations (25 °C for two months). The superior formulations identified based on their physicochemical properties were selected for aerosolization studies, where nebulizers were employed for drug deposition in the NGI stages. Through this process, an ideal formulation and nebulizer combination were identified for maximal ED, FPD, FPF and RF. Lastly, the sustained release profile of the best formulation was also determined in different pH media (mirroring various physiological media) at room temperature.

Materials and methods

Materials

Trans-resveratrol (TR) was purchased from Manchester Organics (Cheshire, UK). Tripalmitin (Dynasan 116) was kindly provided by IOI Oleochemicals (Witten, UK). Glycerol monostearate was obtained from Alfa Aesar, UK. Gelucire 50/13, Compritol 888 ATO and glycol monocaprylate type II (Capryol 90) were generously gifted by Gattefosc (Berkshire, UK). Soya phosphatidylcholine (Lipoid; S-75) was purchased from Lipoid, Switzerland. Tween 80 was procured from Sigma Aldrich, UK. HPLC grade acetonitrile, ammonium molybdate, formic acid, and tetrahydrofuran were purchased from Fischer Scientific Ltd., UK.

Preparation of Nanostructured lipid carriers

Nanostructured lipid carrier (NLC) formulations were prepared *via* hot high-pressure homogenization using three separate phases: the lipid phase, the drug phase and the liquid phase. NLC formulations (F1-F12) were prepared using one liquid lipid (Capryol 90) in combination with four different solid lipids (Dynasan 116, glycerol monostearate, Gelucire 50/13 and Compritol 888), in three different ratios (90:10, 50:50 and 10:90 w/w). Each combination was further prepared using Tween 80 as a surfactant in a 0.5% concentration, where soya phosphatidylcholine (Lipoid; S-75) was employed as a co-surfactant in all NLC formulations (Table 1).

The lipid phase was prepared by weighing Capryol 90 (a liquid lipid) and Dynasan 116 (one of a solid lipid) in a 90:10 w/w ratio (i.e., 1800:200 mg) in a glass beaker (100 ml). Both lipids were melted at 75 °C (approximately 10 °C above their respective phase transition temperatures) *via* a digital hotplate magnetic stirrer (Benchmark Scientific, UK). The same procedure was applied for all other combinations of liquid to solid lipid (Table 1).

The drug phase was prepared, where 500 mg of trans-resveratrol (TR) was dissolved in 10 ml of ethanol (as a stock solution) because the drug is hydrophobic. From this drug phase or stock solution, only 1 ml was taken containing 50 mg of TR for NLCs formulation [42]. An aqueous phase was prepared by mixing tween 80 at 0.5% (i.e., 250 mg) in preheated water (75 °C) (sufficient to prepare a 50 ml formulation) with the aid of a digital hotplate and magnetic stirrer.

Initially, the prepared drug phase was added into the molten lipid phase, followed by the addition of the aqueous phase with continuous stirring for 15 min at 1250 rpm to obtain an emulsion (dispersion system). This dispersion system (microparticles) was homogenized (Ultra-Turax; IKA England Ltd) at 10,000 rpm for 3 min. The resulting microparticles in the dispersion system were then reduced *via* probe sonication (Qsonica probe sonicator, UK) at an amplitude intensity of 60% for a total of 5 min (i.e., 2 min sonication time and 1 min interval time) to obtain TR entrapped in NLCs (TR-NLCs). TR-NLC formulations were then left to cool down to room temperature (25 °C). The resultant TR-NLC formulations were then subjected to bench centrifugation (Eppendorf centrifuge, UK) in order to separate titanium particles (leached out during the sonication process) at a lower centrifugal force of 1250 g for 8 min. Titanium particles sedimented to the bottom of the tube, whereas the suspended nanoparticles in the formulation were separated out. The same formulation steps were repeated for all TR-NLC formulations (Table 1).

Table 1. TR-NLC (F1-F12) formulations prepared comprising of one liquid lipid (Capryol 90) and four solid lipids (Dynasan 116, Glycerol monostearate, Gelucire 50/13 and Compritol 888) in three different w/w ratios (90:10, 50:50 and 10:90), where tween 80 was used as a surfactant (0.5%), and SPC-75 (50 mg) as a co-surfactant. Trans-resveratrol (TR) was employed as the model drug (50 mg) in all formulations.

TR-NLCs particle size and Zeta potential analysis

Particle size and the polydispersity index (PDI) of TR-NLC formulations were measured using a Zetasizer (Malvern Zetasizer Nano series, UK) *via* dynamic light scattering [9, 43]. For analysis, 0.5 ml of TR-NLC formulations were diluted with 10 ml of deionized water, followed by 2 min of vortex mixing (Fisons WhirliMixer, Fisons Scientific Equipments, UK) for uniform particle distribution [42]. Furthermore, following aerosolization of TR-NLC formulations *via* medical nebulizer into the next generation impactor (NGI), each plate was washed with deionized water, and then 2 min of vortex mixing was conducted for uniform mixing and distribution of particles. The Zeta potential of TR-NLC formulations was obtained employing disposable folded capillary cells and using Laser Doppler Velocimetry (LDV) *via* electrophoretic mobility in the aqueous dispersion medium.

Determination drug entrapment efficiency

For the calculation of the entrapment efficiency of TR in the NLC formulations, the total drug and the unentrapped drug were determined. To quantify the total drug, 0.5 ml of the TR-NLC formulations was

mobile phase (as detailed below), followed by processing *via* HPLC (Agilent 1200 series instrument, UK). For the untrapped drug quantification, 0.5 ml of TR-NLC formulations was transferred into a Millipore centrifuge filter (3 kDa; Fisher Scientific, UK), placed into an Eppendorf tube. This tube was then subjected to bench centrifugation (Eppendorf centrifuge, UK) for 15 min at 10000 rpm (i.e., 9300 g), resulting in clear filtrate collected at the bottom of the tube. Whereas TR entrapped in the NLC particles were retained by the filter due to their high molecular weight (only free drug may pass through the filter due to its lower molecular weight). The concentration of TR in the filtrate was determined by HPLC. Thus, the entrapment efficiency (Equation 1) as well as the recovery percentage (Equation 2) of TR in NLC formulations were quantified by the following equations:

$$\text{Entrapment efficiency (\%)} = \frac{\text{Total drug} - \text{Untrapped drug}}{\text{Total drug}} \times 100 \quad (1)$$

$$\text{Recovery (\%)} = \frac{\text{Practical amount of drug obtained from HPLC calibration curve}}{\text{Theoretical amount (amount of drug added during preparation)}} \times 100 \quad (2)$$

An Agilent 1200 series HPLC instrument was used with C-18 column, 4.6 x 250 mm (Phenomenex, UK) with particle size of 5 μm , and the UV detector was set at 306 nm wavelength. The injection volume of 20 μl and the flow rate of 1 ml/min were set up. Two solvents (acetonitrile (A) and 0.1% formic acid in water (B)) were used as the mobile phase with a gradient elution method for 15 min. At 0 minutes, the solvent A ratio was 10% and solvent B was 90%; at 13 min, solvent A was 85% and solvent B was 15%; at 15 min, solvent A was 10% and solvent B was 90%.

Stability studies of TR-NLCs formulations

Preliminary stability studies of TR-NLC formulations were conducted for the following physicochemical properties (i.e., particle size, PDI, Zeta potential and entrapment efficiency) for comparison between freshly prepared TR-NLC formulations and formulations stored at 25 °C for four weeks. The stored TR-NLC formulations were retained in amber-coloured glass bottles (20 ml) and a constant temperature was maintained during the stability studies.

Surface morphology study of TR-NLC formulations

Surface morphology examination of the TR-NLC formulations was conducted *via* transmission electron microscopy (TEM). Two drops of a negative stain ammonium molybdate and two drops of TR-NLC formulation were combined on a glass slide; subsequently, a small drop of the resultant mixture was then placed onto a carbon coated copper grid (400 mesh) (TAAB Laboratories Equipment Ltd., UK). This was then allowed to dry for 2 h. TR-NLC structures were observed, with several images captured *via* a TEM instrument (Morgagni 268, MegaView, UK).

***In-vitro* studies of TR-NLC formulations via nebulization**

A next generation impactor (NGI) (Copley Scientific Limited, UK) was employed for the aerosolization study in combination with medical nebulizers. The NGI was set up by coupling the device with a vacuum pump (Copley flow HCP5, Copley Scientific, UK) and a critical airflow controller (Copley TPK 2000, Copley Scientific, UK) to adjust the airflow rate to 15 L/min. At this airflow rate using an NGI, the aerodynamic cut-off diameters for each stage were calibrated by the manufacturer as; Stage 1 (14.10 μm); Stage 2 (8.61 μm); Stage 3 (5.39 μm); Stage 4 (3.30 μm); Stage 5 (2.08 μm); Stage 6 (1.36 μm); Stage 7 (0.98 μm) and Micro-orifice Collector (<0.70 μm). Prior to aerosolization, the NGI and its stages were refrigerated for 90 min at 5 °C. For the nebulization of TR-NLC formulations, two nebulizers; an air jet (PARI Tourboboy 5 air jet, UK) and an ultrasonic nebulizer (Unicliffe rechargeable ultrasonic inhaler MY-520B, UK) were used. Prior to nebulization, all empty stages were weighed separately. The TR-NLC formulation (3 ml) was then poured into the nebulizer reservoir and weighed. The position of the nebulizer was adjusted in front of the mouthpiece (induction port) of the NGI before starting the aerosolization process. Following total/complete nebulization (i.e., where no further aerosols were generated), the nebulization time (continuous generation of aerosols) and sputtering time (from sporadic to no generation of aerosols) were noted. The mass output and mass output rate were determined with the help of the following equations:

$$\text{Mass output (\%)} = \frac{\text{Weight of nebulized formulation}}{\text{Weight of formulation present in nebulizer before nebulization}} \times 100 \quad (3)$$

$$\text{Mass output rate (mg/min)} = \frac{\text{Weight of nebulized formulation}}{\text{Complete nebulization time}} \quad (4)$$

The emitted dose (ED) is the total amount of TR-NLC formulation released from the nebulizer. Fine particle dose (FPD) is the mass of those particles that are smaller than 5 μm of the ED. Fine particle fraction (FPF) is the fraction of those particles (< 5 μm) connected to the ED, whereas respirable fraction (RF) demonstrates particles that reach the lower respiratory tract. ED, FPD, FPF and RF were calculated with the aid of the below equations.

$$\text{ED (\%)} = \frac{\text{Initial mass in nebulizer} - \text{Final mass remaining in nebulizer}}{\text{Initial mass in nebulizer}} \times 100 \quad (5)$$

$$\text{RF (\%)} = \frac{\text{Fine particle dose}}{\text{Total particle mass on all stages}} \times 100 \quad (6)$$

$$\text{FPD} = \text{Mass deposited on stage 2 through 7} \quad (7)$$

$$\text{FPF (\%)} = \frac{\text{Fine particle dose}}{\text{Initial particle mass loaded in nebulizer}} \times 100 \quad (8)$$

Release study of TR-NLC formulations

The sustained release performance of TR from the NLC formulations (1 mg/1 mL) was evaluated using dialysis tubing (a cut-off MWCO; 3500 Daltons). TR-NLCs formulation (5 ml) were placed in dialysis bags and sealed; these were then sited in a release medium in a dissolution apparatus USP II (Varion instrument, UK). The rotation speed was adjusted to 100 rpm and the temperature condition was maintained at 37 °C. Release studies of TR from NLC formulations were conducted in three different release media: acetate buffer (pH 5), deionized water (pH 7) and phosphate buffer (pH 7.4). Moreover, TR alone (pure drug; 5 mg/5 ml) was also used as a control in each of the release media. 1 ml aliquots were withdrawn from each TR-NLC formulation and control sample from each media at set time intervals (30 min, 1, 2, 3, 4, 5, and 24 h) and replaced with 1 ml of release media (each time). The concentration of TR in each sample was analysed through HPLC and the percentage release of TR was calculated.

Statistical analysis

Analysis of variance (ANOVA) and student's *t*-test were performed using SPSS software for statistical analysis to identify significant differences amongst the data of groups. A *p* value less than 5 was considered to be a significant difference. All formulations were prepared in triplicate and experiments were conducted for each batch separately.

Results and discussion

Initial investigation and selection of TR-NLC formulations

After initial characterization (particle size, PDI, Zeta potential and entrapment efficiency) of both freshly prepared and stored (25 °C for two months) formulations, the best TR-NLC formulations were selected based on these properties. Using Dynasan 116 (Glycerol Tripalmitate) as a solid lipid in F1-F3 TR-NLC formulations, the particle size of freshly prepared and stored formulations exhibited a higher particle size when a higher concentration of solid lipid and a lower concentration of liquid lipid were employed (Table 2). No significant difference ($p > 0.05$) was observed between the F1 and F2 formulations when freshly prepared or even stored. However, when a lower concentration of liquid lipid was employed (i.e., F3), particles showed a significant increase ($p < 0.05$) in size (with a higher amount of Dynasan 116), irrespective of age (i.e., freshly prepared or stored) [44].

These findings are consistent with previous literature, where a large particle size was observed with higher concentrations of Dynasan 116 when compared to a liquid lipid [45]. Both glycerol monostearate (F4-F6) and Gelucire 50/13 (F7-F9) were employed as solid lipids. It was noted that TR-NLC formulations prepared containing these solid lipids with Capryol 90 as a liquid lipid resulted in particle aggregation and demonstrated a significant difference ($p < 0.05$) in particle size when comparison was conducted between freshly prepared and stored formulations (Table 2).

Compritol 888 in TR-NLC formulations (F10-F12) also exhibited a larger particle size when a higher concentration of this solid lipid was employed in TR-NLC formulations. Significantly large particle sizes were observed between the freshly prepared and stored formulations; this may be attributed to the potential interaction of this particular solid lipid with the liquid lipid (Table 2). These results are also in agreement with a study conducted by Bahari and Hamishehkar, when Compritol-based NLCs were prepared and stored at room temperature for 90 days [46]. Similar findings of a resultant large particle size was also noted in NLC formulations when Compritol 888 was utilized as a solid lipid [47]. Moreover, upon increasing the liquid lipid concentration in NLC formulations, a decreasing trend in particle size was observed [48].

Overall, it was observed that, upon increasing solid lipid concentration and reducing liquid lipid concentration, particle size increased in a concentration dependent fashion. Higher concentrations of solid lipid are associated with greater particle crystallinity, resulting in lattices in the lipid core, leading to poor stability and particle aggregation, accounting for the increase in particle size. [49, 50]. A similar trend was observed in terms of PDI for the tested formulations, with stored formulations exhibited higher values than freshly prepared formulations. Trends in particle size were not mirrored in zeta potential. No significant difference ($p > 0.05$) was observed when comparing freshly prepared and stored formulations; moreover, no significant difference ($p > 0.05$) was noted between all TR-NLC tested formulations (Table 2). However, it is important to know that zeta potential is an important parameter and a physical property to determine the surface charges, interaction with surfaces and stability of formulations [51]. In addition, formulations may have different charges based on their composition or surface modifications (i.e., negative, positive or neutral). In general, when colloidal formulations have low zeta potential, they tend to aggregate, affecting their stability. However, particles of NLC formulations tend to repel each other when their zeta potential value is more than ± 30 mV [52], and a similar trend was found for fullerene when their zeta potential values were more than ± 40 mV [53]. Whereas formulations possessing lower charges than these values may be unstable due to the nanoparticles attraction strength becoming greater than the repulsion, which may lead to the disruption of dispersion and subsequently cause agglomeration [54]. Furthermore, even though according to a general stability rule when particles have higher positive or lower charges (± 30 mV), if the density of the particles is greater than the dispersant, they will eventually sediment/aggregate [55].

Amongst the formulations tested, all twelve formulations were identified as possessing high entrapment efficiency [56, 57].

This may be due to the miscibility of TR in the chosen lipids, causing a disruption in the formation of crystal lattices. This may be attributed to the accommodation of high TR loading and solubility in the lipid matrix, leading to higher TR entrapment [58, 59]. Overall, based on the physicochemical properties of TR-NLC formulations and their stability, the following two formulations, F1 and F2 were selected for further characterization.

Table 2. Particle size, polydispersity index (PDI), Zeta potential, and entrapment efficiency of TR-NLC formulations (F1-F12) of freshly prepared formulations and formulations stored at 25 °C for two months. Data are mean \pm SD, n = 3.

Morphology study of TR-NLC formulations *via* transmission electron microscopy (TEM)

TEM was employed to study the surface morphology of selected TR-NLC F1 and F2 formulations. TR-NLC formulations were noted to be spherical in shape and within the nanometer size range (Figure 1). These observations are in agreement with research conducted by Thatipamula et al. [60] when using domperidone-loaded NLCs.

Figure 1. Transmission electron microscope images of TR-NLC formulations (A) F1, and (B) F2. These images are typical of three such different experiments.

Particle size and deposition of TR in NGI stages *via* nebulization

Following the selection of formulations based on physicochemical properties, formulations F1 and F2 were selected for aerosolization performance using air jet and ultrasonic nebulizers in the next generation impactor (NGI). Upon aerosolization *via* an air jet nebulizer, significantly ($p < 0.05$) larger particles were deposited in stages 1-2 of the NGI, whereas smaller particles were deposited in stages 3-5 for both F1 and F2 formulations (Figure 2 A). This trend was observed for both formulations and may be attributed to the design of the nebulizer, which was deemed to minimally impact the formulation. Moreover, the air jet nebulizer possesses a baffle, allowing for smaller droplet formation for inhalation and retaining larger droplets by impacting upon the baffle, deflecting the formulation back into the reservoir for re-aerosolization. The larger particle sizes observed in the initial 1-2 stages of the NGI may be attributed to the high velocity of compressed air, which causes the formulation to deposit in the initial stages *via* inertial impaction. However, based on droplet size, smaller droplets may be propelled a greater distance in the NGI and hence produce high drug deposition in the latter stages of the model. This was also confirmed *via* TR drug deposition, demonstrating significantly high ($p < 0.05$) drug deposition in the middle to lower stages of NGI (i.e., stages 3-5 (Figure 2 C)).

Ultrasonic nebulizers possess a piezoelectric crystal that generates vibration in formulation suspension. The distance between aerosol generation and baffle location is quite large, and therefore the baffle cannot retain all large droplets. Thus, the deposition of the formulation in the different stages of the NGI is proposed to be dependent on the particle size.

TR-NLC formulation F2 exhibited a significantly larger ($p < 0.05$) particle size in the early stages of the NGI (Stages 1-4) when compared to stages 5-8 (Figure 2 B). Whereas formulation F1 demonstrated significantly larger particle size in stages 1-2, upon comparing to other stages (i.e., 3-8) in the NGI. The larger particle size deposited in the earlier stages for TR-NLC formulations F1 and F2 demonstrated high drug deposition in these stages. Drug deposition was determined to be directly related to the particle size (i.e., large size resulting in lower deposition) and hence related to the design of the nebulizer producing large droplets (Figure 2 B and Figure 2 D). Comparisons of deposition based on the nebulizer type identified the air jet nebulizer as possessing overall superior performance (higher deposition in the later stages indicating deep lung deposition) when compared to the ultrasonic nebulizer.

Figure 2. Aerosolization of TR-NLC formulations F1 and F2 via air jet nebulizer for (A and B) particle size (nm), and (C and D) TR deposition in various stages of the NGI. Air jet and ultrasonic nebulizers demonstrated particle size and drug deposition in the NGI stages using an airflow rate of 15 L/min. Data are mean \pm SD, n = 3.

Aerosolization performance of TR-NLC formulations

After complete nebulization, the TR-NLC F1 formulation showed significantly higher ($p < 0.05$) ED when nebulized using both the air jet ($87.44 \pm 3.36\%$) and ultrasonic ($64.28 \pm 3.52\%$) nebulizers, when compared to the TR-NLC F2 formulation (Table 3). However, the air jet nebulizer emitted a significantly higher ($p < 0.05$) amount of formulation than the ultrasonic nebulizer. ED represents the amount of TR-NLC formulation emitted from the nebulizer and deposited in various stages of the NGI. The higher ED when combined with the air jet nebulizer is attributed to the lower amount of formulation retained in the nebulizer reservoir, referred to as “dead/residual volume” after complete nebulization time, when compared to the ultrasonic nebulizer. Similar to ED, the TR-NLC F1 formulation showed significantly higher ($p < 0.05$) FPD when compared to the TR-NLC F2 formulation, irrespective of the nebulizer type used (Table 3). FPD represents the deposition of TR in the various stages (i.e., stages 2-7) of the NGI. Using an airflow rate of 15 L/min in the air jet nebulizer, higher ($p < 0.05$) TR deposition was observed for the F1 formulation ($1652.52 \pm 9.68 \mu\text{g}$) in comparison to the F2 formulation ($1010.56 \pm 8.27 \mu\text{g}$), whereas when the ultrasonic nebulizer was employed, a significantly lower TR deposition in the NGI stages (Table 3) was observed in comparison to the air jet nebulized formulations.

The trend of higher FPD is closely related to the ED, as the air jet nebulizer was noted to retain lower concentrations of TR-NLC formulation post-aerosolization, whereas a higher dead volume was retained by the ultrasonic nebulizer [50]. FPF is the fraction of formulation particles that are smaller than $5 \mu\text{m}$ and deposited in stages 2-7 of the NGI from the ED. Upon analysis, a higher FPF was also found for the air jet nebulizer when compared to the ultrasonic nebulizer (Table 3). These results are in concordance with the previous research that demonstrated high FPF for air jet nebulizers [50, 61].

RF is the fraction of droplets that are less than 5 μm deposited in the stages of NGI [38]. The air jet nebulizer deposited a high volume of RF for both TR-NLC F1 and F2 formulations when compared to the ultrasonic nebulizer (Table 3). This may be attributed to the generation of smaller droplets by the air jet nebulizer, where the baffle is located just above the venturi nozzle and may result in the formation of smaller droplets for inhalation (i.e., higher drug deposition in the lower stages of the NGI), whereas larger droplets impact on the baffle (may further generate smaller droplets) and deflect back the formulation to the reservoir for re-aerosolization. This phenomenon is not efficient in the ultrasonic nebulizer, and therefore both smaller and larger droplets are readily available for inhalation, consequently leading to larger droplet deposition in the earlier stages of the NGI (i.e., induction port and stage 1) due to inertial impaction. Larger droplets and their deposition in the earlier stages of the NGI represent higher drug deposition in the upper stages, whereas lower droplet sizes allow desirable deposition in the lateral stages. Overall, post-aerosolization of TR-NLC F1 and F2 formulations, it was found that the air jet nebulizer in combination with the F1 formulation resulted in the highest drug deposition in the lower stages of the NGI.

Table 3. Aerosolization performance using an air jet and ultrasonic nebulizers employing TR-NLCs F1 and F2 formulations in a next generation impactor (NGI) at an airflow rate of 15 L/min for the determination of emitted dose (ED), fine particle dose (FPD), fine particle fraction (FPF) and respirable fraction (RF). Data are mean \pm SD, n = 3.

***In-vitro* release study of TRES-NLCs F14 formulation**

For sustained release, TR alone was used as a control, and 100% of the release was found after 4 hours (data not shown). However, over a period of 8 h, the maximum release of TR was found in the TR-NLC F1 formulation ($p < 0.05$) when compared to the TR-NLC F2 formulation, regardless of the dissolution media type (Figure 3). A trend of higher to lower release of TR from NLC formulations (F1 and F2) was found depending on media as follows: acetate buffer > water > phosphate buffer. Moreover, the F1 and F2 formulations demonstrated the highest ($29.73 \pm 0.76\%$ and $25.87 \pm 0.81\%$) and lowest ($15.95 \pm 0.69\%$ and $12.72 \pm 0.84\%$) release of TR ($p < 0.05$) in acetate and phosphate buffer (Figure 3). It is noteworthy that the highest release of drug in acetate buffer may be attributed to the acidic medium of the media (pH 5.4), which retains TR stability when compared to alternative media, protecting the hydroxyl group of TR from radical oxidation (i.e., *via* positively charged H_3O^+) [62]. Whereas the basic media may make TR unstable, due to its hydrolysis and degradation. Similarly, previous research has indicated TR stability in an acidic medium, with the stability of the drug decreasing with increasing pH [63, 64]. It is important to know that the low level of oxygen in cancer may cause a metabolic shift and hence generate an acidic environment [65], and therefore these formulations were investigated in different pH environments to assess the release profile of TR. Thus, the selection of dissolution media has a major effect on TR stability and its release profile.

Figure 3. Sustained release of TR as a model drug from TR-NLCs formulations F1 (solid lines) and F2 (dotted lines), employing three dissolution media, including acetate buffer (pH 5.4), water (pH 7), and phosphate buffer (pH 7.4). Data are mean \pm SD, n = 3.

Conclusion

In this study, TR-NLC formulations (F1-F12) were designed and prepared employing one liquid lipid (Capryol 90), four solid lipids (Dynasan 116, glycerol monostearate, Gelucire 50/13 and Compritol 888) in two different ratios (90:10 and 50:50 w/w), tween 80 and SPC S-75 as a surfactant and a co-surfactant. After post-physicochemical properties characterization and stability studies at 25 °C for two months (including smaller particle size, lower values of PDI, Zeta potential and higher entrapment efficiency of TR), only TR-NLC formulations F1 and F2 were selected for further studies. Both formulations characterized as nanoformulations with associated particle sizes falling within the nanometric range, were also confirmed *via* TEM. Upon aerosolization, the F1 formulation demonstrated smaller particle size and higher TR deposition in the middle to lower stages of the NGI when an air jet nebulizer was used, as compared to the F2 formulation *via* an ultrasonic nebulizer. Moreover, aerosolization performance was also superior when a combination of air jet nebulizer and F1 formulation was employed, producing higher ED, FPD, FPF and RF. Thus, this combination of formulation and nebulizer may possess enhanced suitability for delivering drug formulation into the lateral stages of the pulmonary system.

CRedit authorship contribution statement

Iftikhar Khan: Project administration, Conceptualization, Supervision, Writing - Review & Editing.

Maria Sabu: Writing - Original draft preparation, Data curation, Methodology. **Nozad Hussein:** Data

curation, Software. **Huner Omer:** Methodology, Visualization. **Chahinez Houacine:** Software,

Methodology, Investigation. **Wasiq Khan:** Software, Investigation. **Abdelbary Elhissi:** Writing -

Review & Editing, Investigation. **Sakib Yousaf:** Visualization, Writing - Review & Editing.

Declaration of Interest

The authors declare no conflict of interest.

References

1. E. Fröhlich, A. Mercuri, S. Wu and S. Salar-Behzadi. Measurements of deposition, lung surface area and lung fluid for simulation of inhaled compounds. *Frontiers in Pharmacology*, 7 (2016)
2. I. Khan, A. Elhissi, M. Shah, M.A. Alhnan and W. Ahmed. "9 - liposome-based carrier systems and devices used for pulmonary drug delivery." In *Biomaterials and medical tribology*. J. P. Davim. 1. Woodhead Publishing, 2013, 395-443.
3. S. Kumar, A.K. Sharma, H. Lahlhenmawia and D. Kumar. Natural compounds targeting major signaling pathways in lung cancer. *Targeting Cellular Signalling Pathways in Lung Diseases*, (2021) 821-46.
4. C. Fitzmaurice, D. Dicker, A. Pain, H. Hamavid, M. Moradi-Lakeh, M.F. MacIntyre, C. Allen, G. Hansen, R. Woodbrook and C. Wolfe. The global burden of cancer 2013. *JAMA oncology*, 1 (2015) 505-27.
5. F. Bray, J. Ferlay, I. Soerjomataram, R.L. Siegel, L.A. Torre and A. Jemal. Global cancer statistics 2018: Globocan estimates of incidence and mortality worldwide for 36 cancers in 185 countries. *CA: a cancer journal for clinicians*, 68 (2018) 394-424.
6. R.S. Herbst, D. Morgensztern and C. Boshoff. The biology and management of non-small cell lung cancer. *Nature*, 553 (2018) 446-54.
7. E.A. Semenova, R. Nagel and A. Berns. Origins, genetic landscape, and emerging therapies of small cell lung cancer. *Genes & development*, 29 (2015) 1447-62.
8. S. Zhang, R. Li, T. Jiang, Y. Gao, K. Zhong, H. Cheng, X. Chen and S. Li. Inhalable nanomedicine for lung cancer treatment. *Smart Materials in Medicine*, 5 (2024) 261-80.
9. S.S. Yousaf, A. Isreb, I. Khan, E. Mewsiga, A. Elhissi, W. Ahmed and M.A. Alhnan. Impact of nanosizing on the formation and characteristics of polymethacrylate films: Micro- versus nano-suspensions. *Pharmaceutical Development and Technology*, 26 (2021) 729-39.
10. C. Houacine, S.S. Yousaf, I. Khan, R.K. Khurana and K.K. Singh. Potential of natural biomaterials in nano-scale drug delivery. *Curr Pharm Des*, 24 (2018) 5188-206.
11. T.M. Zaccaron, M. Silva, M.P. Costa, D.M.E. Silva, A.C. Silva, A.C.M. Apolônio, R.L. Fabri, F. Pittella, H.V.A. Rocha and G.D. Tavares. Advancements in chitosan-based nanoparticles for pulmonary drug delivery. *Polymers (Basel)*, 15 (2023)
12. E.F. Craparo, S.E. Drago, G. Costabile, M. Ferraro, E. Pace, R. Scaffaro, F. Ungaro and G. Cavallaro. Sustained-release powders based on polymer particles for pulmonary delivery of beclomethasone dipropionate in the treatment of lung inflammation. *Pharmaceutics*, 15 (2023) 1248.
13. S. Kim, S. Park, D.J. Fesenmeier and Y.-Y. Won. Excipient-free lyophilization of block copolymer micelles for potential lung surfactant therapy applications. *International Journal of Pharmaceutics*, 646 (2023) 123476.
14. J. Kaur, M. Gulati, L. Corrie, A. Awasthi, N.K. Jha, D.K. Chellappan, G. Gupta, R. MacLoughlin, B.G. Oliver, K. Dua, *et al.* Role of nucleic acid-based polymeric micelles in treating lung diseases. *Nanomedicine*, 17 (2022) 1951-60.
15. J. Glover, S. Yousaf and I. Khan. "Oral lipid-based carriers: Overcoming the challenges associated with conventional treatments of non-small cell lung cancer." In *Science and applications of nanoparticles*. New York (NY): Jenny Stanford Publishing, 2022, 277-307.
16. M. Ansam, S. Yousaf, R. Bnyan and I. Khan. Anti-aging liposomal formulation. Mini review. *Novel Approaches in Drug Designing and Development*, 3 (2018) 66-68.
17. I. Khan, A. Al-Hasani, M.H. Khan, A.N. Khan, F.E. Alam, S.K. Sadozai, A. Elhissi, J. Khan and S. Yousaf. Impact of dispersion media and carrier type on spray-dried proliposome powder formulations loaded with beclomethasone dipropionate for their pulmonary drug delivery via a next generation impactor. *PLoS One*, 18 (2023) e0281860.

18. N.A.N. Hanafy, R.H. Abdelbadea, A.E. Abdelaziz and E.A. Mazyed. Formulation and optimization of folate-bovine serum albumin-coated ethoniosomes of pterostilbene as a targeted drug delivery system for lung cancer: In vitro and in vivo demonstrations. *Cancer Nanotechnology*, 14 (2023) 49.
19. K. Sudhakar, V. Mishra, S. Jain, N.C. Rompicherla, N. Malviya and M.M. Tambuwala. Development and evaluation of the effect of ethanol and surfactant in vesicular carriers on lamivudine permeation through the skin. *International Journal of Pharmaceutics*, 610 (2021) 121226.
20. R. Bnyan, I. Khan, T. Ehtezazi, I. Saleem, S. Gordon, F. O'Neill and M. Roberts. Formulation and optimisation of novel transfersomes for sustained release of local anaesthetic. *Journal of Pharmacy and Pharmacology*, 71 (2019) 1508-19.
21. I. Khan, M. Apostolou, R. Bnyan, C. Houacine, A. Elhissi and S.S. Yousaf. Paclitaxel-loaded micro or nano transfersome formulation into novel tablets for pulmonary drug delivery via nebulization. *International Journal of Pharmaceutics*, 575 (2020) 118919.
22. K.R. Gajbhiye, R. Salve, M. Narwade, A. Sheikh, P. Kesharwani and V. Gajbhiye. Lipid polymer hybrid nanoparticles: A custom-tailored next-generation approach for cancer therapeutics. *Molecular Cancer*, 22 (2023) 160.
23. A. Wadhwa, T.R. Bobak, L. Bohrmann, R. Geczy, S. Sekar, G. Sathyanarayanan, J.P. Kutter, H. Franzzyk, C. Foged, K. Saatchi, *et al.* Pulmonary delivery of sirna-loaded lipid-polymer hybrid nanoparticles: Effect of nanoparticle size. *OpenNano*, 13 (2023) 100180.
24. M.J. Altube, N. Perez, E.L. Romero, M.J. Morilla, L.H. Higa and A.P. Perez. Inhaled lipid nanocarriers for pulmonary delivery of glucocorticoids: Previous strategies, recent advances and key factors description. *Int J Pharm*, 642 (2023) 123146.
25. J. German-Cortés, M. Vilar-Hernández, D. Rafael, I. Abasolo and F. Andrade. Solid lipid nanoparticles: Multitasking nano-carriers for cancer treatment. *Pharmaceutics*, 15 (2023)
26. M. Apostolou, S. Assi, A.A. Fatokun and I. Khan. The effects of solid and liquid lipids on the physicochemical properties of nanostructured lipid carriers. *Journal of Pharmaceutical Sciences*, 10 (2021) 2859-72.
27. S. Ahalwat, D.C. Bhatt, S. Rohilla, V. Jogpal, K. Sharma, T. Virmani, G. Kumar, A. Alhalmi, A.S. Alqahtani, O.M. Noman, *et al.* Mannose-functionalized isoniazid-loaded nanostructured lipid carriers for pulmonary delivery: In vitro prospects and in vivo therapeutic efficacy assessment. *Pharmaceutics (Basel)*, 16 (2023)
28. B. García-Pinel, C. Porras-Alcalá, A. Ortega-Rodríguez, F. Sarabia, J. Prados, C. Melguizo and J.M. López-Romero. Lipid-based nanoparticles: Application and recent advances in cancer treatment. *Nanomaterials*, 9 (2019) 638.
29. N.I. Payne, P. Timmins, C.V. Ambrose, M.D. Ward and F. Ridgway. Proliposomes: A novel solution to an old problem. *J Pharm Sci*, 75 (1986) 325-9.
30. H. Chahinez, K. Iftikhar and Y. Sakib Saleem. Potential cardio-protective agents: A resveratrol review (2000-2019). *Current Pharmaceutical Design*, 26 (2020) 1-16.
31. H. Wu, L. Chen, F. Zhu, X. Han, L. Sun and K. Chen. The cytotoxicity effect of resveratrol: Cell cycle arrest and induced apoptosis of breast cancer 4t1 cells. *Toxins (Basel)*, 11 (2019)
32. V.K. Bhaskara, B. Mittal, V.V. Mysorekar, N. Amaresh and J. Simal-Gandara. Resveratrol, cancer and cancer stem cells: A review on past to future. *Current Research in Food Science*, 3 (2020) 284-95.
33. D.J. Boocock, G.E. Faust, K.R. Patel, A.M. Schinas, V.A. Brown, M.P. Ducharme, T.D. Booth, J.A. Crowell, M. Perloff and A.J. Gescher. Phase i dose escalation pharmacokinetic study in healthy volunteers of resveratrol, a potential cancer chemopreventive agent. *Cancer Epidemiology Biomarkers & Prevention*, 16 (2007) 1246-52.

34. V.A. Brown, K.R. Patel, M. Viskaduraki, J.A. Crowell, M. Perloff, T.D. Booth, G. Vasilinin, A. Sen, A.M. Schinas and G. Piccirilli. Repeat dose study of the cancer chemopreventive agent resveratrol in healthy volunteers: Safety, pharmacokinetics, and effect on the insulin-like growth factor axis. *Cancer research*, 70 (2010) 9003-11.
35. W. Zhu, W. Qin, K. Zhang, G.E. Rottinghaus, Y.-C. Chen, B. Kliethermes and E.R. Sauter. Trans-resveratrol alters mammary promoter hypermethylation in women at increased risk for breast cancer. *Nutrition and cancer*, 64 (2012) 393-400.
36. I. Khan, S. Yousaf, M.A. Alhnan, W. Ahmed, A. Elhissi and M.J. Jackson. "Design characteristics of inhaler devices used for pulmonary delivery of medical aerosols." In *Surgical tools and medical devices*. W. Ahmed and M. J. Jackson. Cham: Springer International Publishing, pp: 573-591, 2016, 573-91.
37. S.A. Shoyele and A. Slowey. Prospects of formulating proteins/peptides as aerosols for pulmonary drug delivery. *Int J Pharm*, 314 (2006) 1-8.
38. C. O'Callaghan and P.W. Barry. The science of nebulised drug delivery. *Thorax*, 52 Suppl 2 (1997) S31-44.
39. A. Elhissi and K.M.G. Taylor. Delivery of liposomes generated from pro liposomes using air-jet, ultrasonic and vibrating-mesh nebulisers. *J. Drug Del. Sci. Technol.*, 15 (2005) 261-65.
40. A. Ari. Jet, ultrasonic, and mesh nebulizers: An evaluation of nebulizers for better clinical outcomes. *Eurasian J Pulmonol*, 16 (2014) 1-7.
41. X. Zhang, Q. Liu, J. Hu, L. Xu and W. Tan. An aerosol formulation of r-salbutamol sulfate for pulmonary inhalation. *Acta Pharm Sin B*, 4 (2014) 79-85.
42. I. Khan, S. Sunita, N.R. Hussein, H.K. Omer, A. Elhissi, C. Houacine, W. Khan, S. Yousaf and H.A. Rathore. Development and characterization of novel combinations and compositions of nanostructured lipid carrier formulations loaded with trans-resveratrol for pulmonary drug delivery. *Pharmaceutics*, 16 (2024) 1589.
43. E. Lason, E. Sikora and J. Ogonowski. Influence of process parameters on properties of nanostructured lipid carriers (nlc) formulation. *Acta Biochim Pol*, 60 (2013) 773-7.
44. N. Dudhipala and A.A. Ay. Amelioration of ketoconazole in lipid nanoparticles for enhanced antifungal activity and bioavailability through oral administration for management of fungal infections. *Chemistry and Physics of Lipids*, 232 (2020) 104953.
45. E.B. Souto, S.A. Wissing, C.M. Barbosa and R.H. Müller. Development of a controlled release formulation based on sln and nlc for topical clotrimazole delivery. *Int J Pharm*, 278 (2004) 71-7.
46. L. Azhar Shekoufeh Bahari and H. Hamishehkar. The impact of variables on particle size of solid lipid nanoparticles and nanostructured lipid carriers; a comparative literature review. *Adv Pharm Bull*, 6 (2016) 143-51.
47. Y.-P. Fang, Y.-K. Lin, Y.-H. Su and J.-Y. Fang. Tryptanthrin-loaded nanoparticles for delivery into cultured human breast cancer cells, mcf7: The effects of solid lipid/liquid lipid ratios in the inner core. *Chemical and Pharmaceutical Bulletin*, 59 (2011) 266-71.
48. E.H. Gokce, E. Korkmaz, E. Deller, G. Sandri, M.C. Bonferoni and O. Ozer. Resveratrol-loaded solid lipid nanoparticles versus nanostructured lipid carriers: Evaluation of antioxidant potential for dermal applications. *International journal of nanomedicine*, (2012) 1841-50.
49. J.P. Barbosa, A.R. Neves, A.M. Silva, M.A. Barbosa, M.S. Reis and S.G. Santos. Nanostructured lipid carriers loaded with resveratrol modulate human dendritic cells. *Int J Nanomedicine*, 11 (2016) 3501-16.
50. I. Khan, S. Hussein, C. Houacine, S. Khan Sadozai, Y. Islam, R. Bnyan, A. Elhissi and S. Yousaf. Fabrication, characterization and optimization of nanostructured lipid carrier formulations using beclomethasone dipropionate for pulmonary drug delivery via medical nebulizers. *International Journal of Pharmaceutics*, 598 (2021) 120376.

51. S. Siva, J.O. Jin, I. Choi and M. Kim. Nanoliposome based biosensors for probing mycotoxins and their applications for food: A review. *Biosensors & bioelectronics*, 219 (2022) 114845.
52. R.J. Hunter, B.R. Midmore and H. Zhang. Zeta potential of highly charged thin double-layer systems. *Journal of Colloid and Interface Science*, 237 (2001) 147-49.
53. D.G. Deryabin, L.V. Efremova, A.S. Vasilchenko, E.V. Saidakova, E.A. Sizova, P.A. Troshin, A.V. Zhilenkov and E.A. Khakina. A zeta potential value determines the aggregate's size of penta-substituted [60]fullerene derivatives in aqueous suspension whereas positive charge is required for toxicity against bacterial cells. *J Nanobiotechnology*, 13 (2015) 50.
54. H. Simunkova, P. Pessenda-Garcia, J. Wosik, P. Angerer, H. Kronberger and G.E. Nauer. The fundamentals of nano- and submicro-scaled ceramic particles incorporation into electrodeposited nickel layers: Zeta potential measurements. *Surface and Coatings Technology*, 203 (2009) 1806-14.
55. R.J. Hunter. *Zeta potential in colloid science: Principles and applications*. London, UK: Academic Press Inc, 1981, 11-55.
56. C. Houacine, D. Adams and K.K. Singh. Impact of liquid lipid on development and stability of trimyristin nanostructured lipid carriers for oral delivery of resveratrol. *Journal of Molecular Liquids*, 316 (2020) 113734.
57. A. Mathew Thevarkattil, S. Yousaf, C. Houacine, W. Khan, R. Bnyan, A. Elhissi and I. Khan. Anticancer drug delivery: Investigating the impacts of viscosity on lipid-based formulations for pulmonary targeting. *International Journal of Pharmaceutics*, 664 (2024) 124591.
58. F.-Q. Hu, S.-P. Jiang, Y.-Z. Du, H. Yuan, Y.-Q. Ye and S. Zeng. Preparation and characteristics of monostearin nanostructured lipid carriers. *International Journal of Pharmaceutics*, 314 (2006) 83-89.
59. A.R. Neves, S. Martins, M.A. Segundo and S. Reis. Nanoscale delivery of resveratrol towards enhancement of supplements and nutraceuticals. *Nutrients*, 8 (2016) 131.
60. R. Thatipamula, C. Palem, R. Gannu, S. Mudragada and M. Yamsani. Formulation and in vitro characterization of domperidone loaded solid lipid nanoparticles and nanostructured lipid carriers. *Daru : journal of Faculty of Pharmacy, Tehran University of Medical Sciences*, 19 (2011) 23-32.
61. M.E. Abdelrahim. Aerodynamic characteristics of nebulized terbutaline sulphate using the andersen cascade impactor compared to the next generation impactor. *Pharmaceutical Development and Technology*, 16 (2011) 137-45.
62. Š. Zupančič, Z. Lavrič and J. Kristl. Stability and solubility of trans-resveratrol are strongly influenced by pH and temperature. *Eur J Pharm Biopharm*, 93 (2015) 196-204.
63. A. Konopko and G. Litwinienko. Unexpected role of pH and microenvironment on the antioxidant and synergistic activity of resveratrol in model micellar and liposomal systems. *J Org Chem*, 87 (2022) 1698-709.
64. T. Pentek, E. Newenhouse, B. O'Brien and A.S. Chauhan. Development of a topical resveratrol formulation for commercial applications using dendrimer nanotechnology. *Molecules*, 22 (2017)
65. J. Chiche, M.C. Brahim-Horn and J. Pouysségur. Tumour hypoxia induces a metabolic shift causing acidosis: A common feature in cancer. *J Cell Mol Med*, 14 (2010) 771-94.

Table1. TR-NLC (F1-F12) formulations prepared comprising of one liquid lipid (Capryol 90) and four solid lipids (Dynasan 116, Glycerol monostearate, Gelucire 50/13 and Compritol 888) in three different w/w ratios (90:10, 50:50 and 10:90), where tween 80 was used as a surfactant (0.5%), and SPC-75 (50 mg) as a co-surfactant. Trans-resveratrol (TR) was employed as the model drug (50 mg) in all formulations.

Formulations	Liquid lipid (mg)	Solid lipid (mg)	Liquid lipid : Solid lipid (w/w)	Tween-80%	Co-surfactant (mg)	TRES (mg)
F1	Capryol 90	Dynasan 116	90:10	0.5	50	50
F2	Capryol 90	Dynasan 116	50:50	0.5	50	50
F3	Capryol 90	Dynasan 116	10:90	0.5	50	50
F4	Capryol 90	Glycerol Monostearate	90:10	0.5	50	50
F5	Capryol 90	Glycerol Monostearate	50:50	0.5	50	50
F6	Capryol 90	Glycerol Monostearate	10:90	0.5	50	50
F7	Capryol 90	Gelucire 50/13	90:10	0.5	50	50
F8	Capryol 90	Gelucire 50/13	50:50	0.5	50	50
F9	Capryol 90	Gelucire 50/13	10:90	0.5	50	50
F10	Capryol 90	Compritol 888	90:10	0.5	50	50
F11	Capryol 90	Compritol 888	50:50	0.5	50	50
F12	Capryol 90	Compritol 888	10:90	0.5	50	50

Table 2. Particle size, polydispersity index (PDI), Zeta potential, and entrapment efficiency of TR-NLC formulations (F1-F12) of freshly prepared formulations and formulations stored at 25 °C for two months. Data are mean \pm SD, n = 3.

Formulations	Particle size (nm)		PDI		Zeta potential (mV)		Entrapment efficiency (%)	
	After preparation	After 2 months	After preparation	After 2 months	After preparation	After 2 months	After preparation	After 2 months
F1	170.65 \pm 13.15	173.65 \pm 8.31	0.22 \pm 0.05	0.20 \pm 0.03	-	-	95.45 \pm 4.3	95.61 \pm 6.71
F2	182.45 \pm 4.31	181.05 \pm 7.81	0.24 \pm 0.03	0.24 \pm 0.04	-	-	93.65 \pm 5.6	94.96 \pm 4.64
F3	412.46 \pm 11.72	562.13 \pm 10.36	0.38 \pm 0.07	0.36 \pm 0.05	-	-	92.75 \pm 7.3	90.89 \pm 7.44
F4	223.28 \pm 7.91	423.48 \pm 8.06	0.38 \pm 0.08	0.32 \pm 0.05	-	-	92.83 \pm 5.7	90.33 \pm 5.68
F5	254.72 \pm 8.98	724.76 \pm 10.52	0.62 \pm 0.07	0.73 \pm 0.08	-	-	86.27 \pm 6.2	84.04 \pm 6.89
F6	362.44 \pm 9.85	681.11 \pm 11.41	0.57 \pm 0.06	0.69 \pm 0.06	-	-	88.49 \pm 7.1	84.68 \pm 7.43
F7	112.65 \pm 4.73	601.27 \pm 7.36	0.46 \pm 0.11	0.59 \pm 0.07	-	-	97.65 \pm 8.6	94.59 \pm 7.06
F8	136.99 \pm 7.21	596.26 \pm 9.06	0.57 \pm 0.05	0.65 \pm 0.09	-	-	94.55 \pm 5.4	90.95 \pm 8.16
F9	174.45 \pm 13.25	599.85 \pm 7.35	0.61 \pm 0.04	0.64 \pm 0.14	-	-	96.74 \pm 7.3	95.97 \pm 7.43
F10	244.38 \pm 18.92	446.75 \pm 12.71	0.45 \pm 0.06	0.56 \pm 0.07	-	-	94.17 \pm 6.6	94.35 \pm 6.12
F11	371.67 \pm 13.05	536.63 \pm 8.62	0.94 \pm 0.06	1.00 \pm 0.04	-	-	91.45 \pm 7.6	91.72 \pm 7.63
F12	549.35 \pm 13.62	668.94 \pm 7.28	0.69 \pm 0.05	0.77 \pm 0.04	-	-	93.05 \pm 5.1	90.61 \pm 6.44

Table 3. Aerosolization performance using an air jet and ultrasonic nebulizers employing TR-NLCs F1 and F2 formulations in a next generation impactor (NGI) at an airflow rate of 15 L/min for the determination of emitted dose (ED), fine particle dose (FPD), fine particle fraction (FPF) and respirable fraction (RF). Data are mean \pm SD, n = 3.

Formulations	ED (%)	FPD (μg)	FPF (%)	RF (%)
F1 Air jet	87.44 \pm 3.36	1652.52 \pm 9.68	36.25 \pm 4.26	93.41 \pm 4.03
F1 Ultrasonic	64.28 \pm 3.52	679.38 \pm 10.66	13.38 \pm 3.51	82.21 \pm 3.34
F2 Air jet	69.35 \pm 2.68	1010.56 \pm 8.27	31.56 \pm 4.82	90.26 \pm 3.27
F2 Ultrasonic	51.72 \pm 3.74	454.54 \pm 9.06	11.63 \pm 3.02	78.54 \pm 3.16

Figure 1

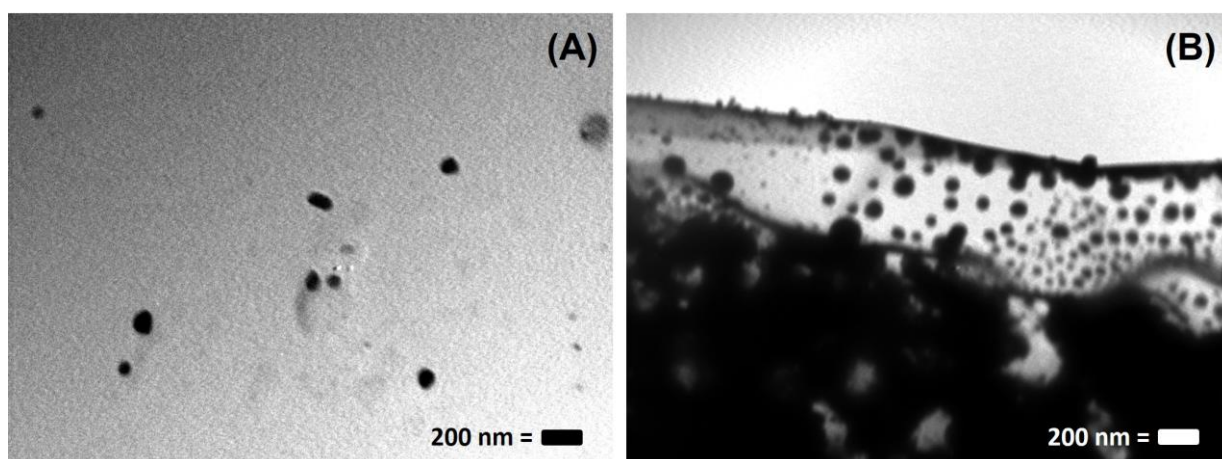


Figure 1. Transmission electron microscope images of TR-NLC formulations (A) F1, and (B) F2. These images are typical of three such different experiments.

Figure 2

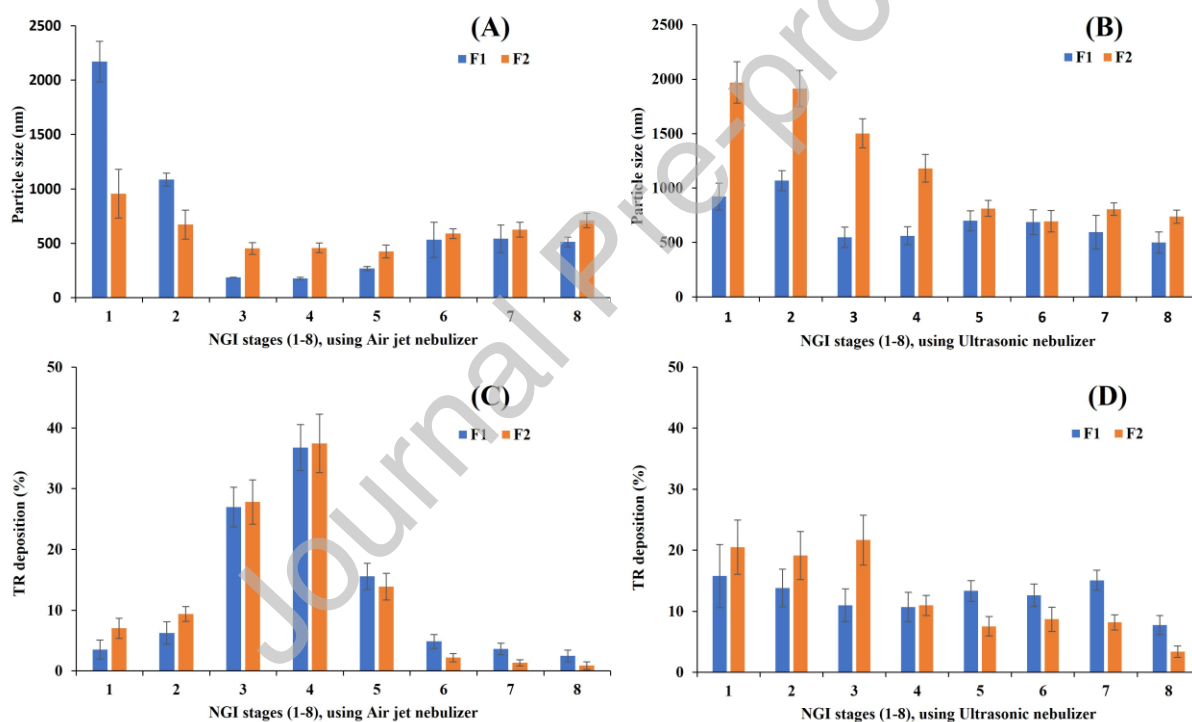


Figure 2. Aerosolization of TR-NLC formulations F1 and F2 *via* air jet nebulizer for (A and B) particle size (nm), and (C and D) TR deposition in various stages of the NGI. Air jet and ultrasonic nebulizers demonstrated particle size and drug deposition in the NGI stages using an airflow rate of 15 L/min. Data are mean \pm SD, n = 3.

Figure 3

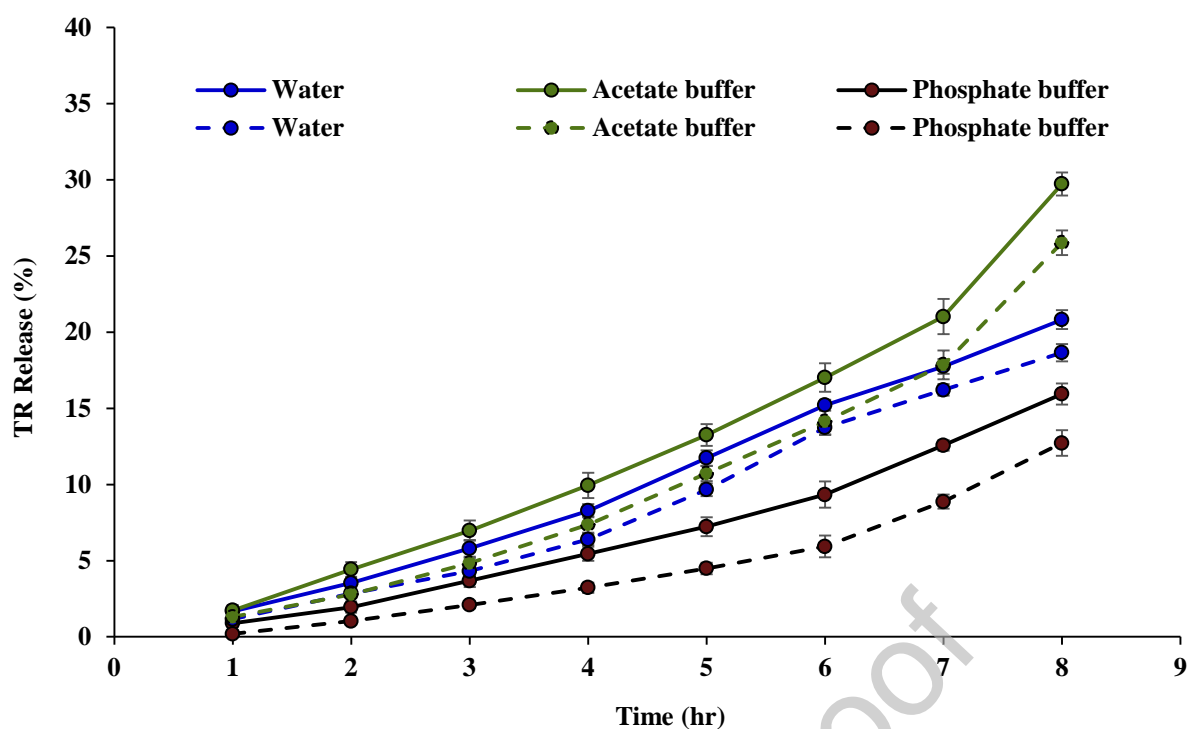
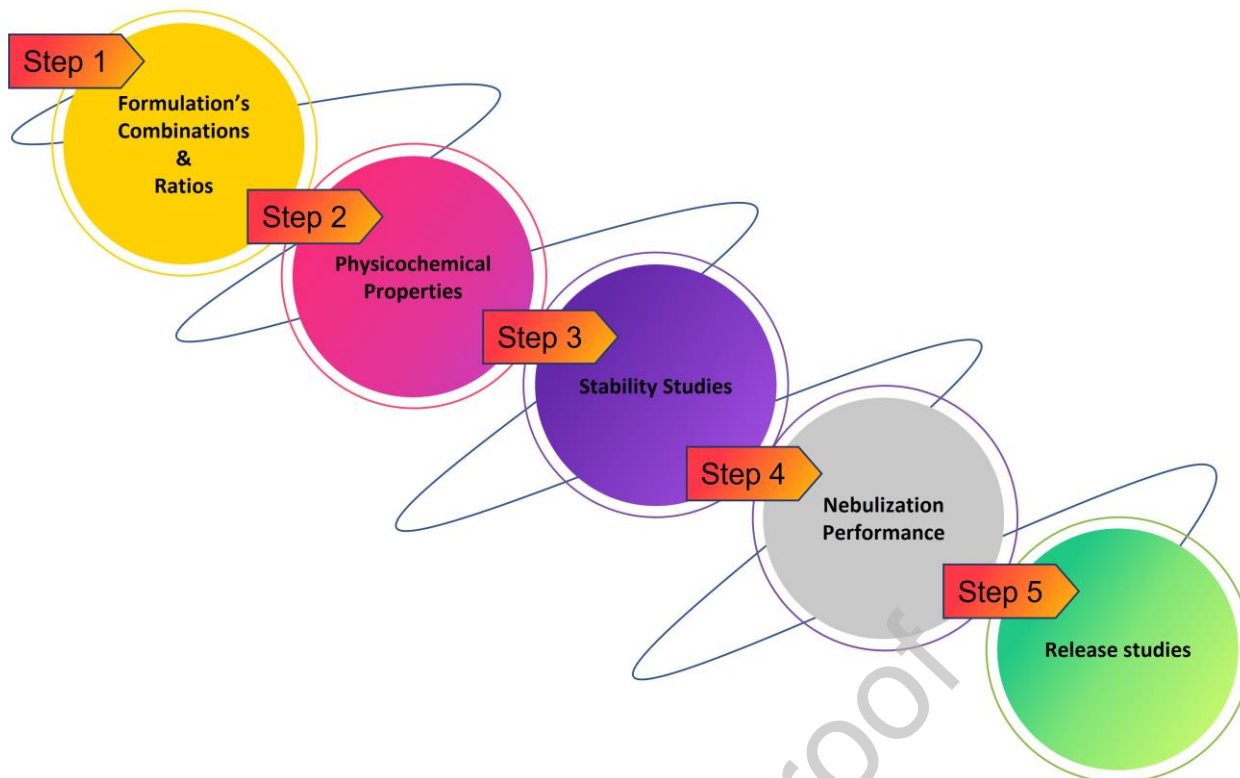


Figure 3. Sustained release of TR as a model drug from TR-NLCs formulations F1 (solid lines) and F2 (dotted lines), employing three dissolution media, including acetate buffer (pH 5.4), water (pH 7), and phosphate buffer (pH 7.4). Data are mean \pm SD, n = 3.



Declaration of interests

The authors declare that they have no known competing financial interests or personal relationships that could have appeared to influence the work reported in this paper.

The authors declare the following financial interests/personal relationships which may be considered as potential competing interests: